Enhanced cell viability in hyaluronic acid coated poly(lactic-co-glycolic acid) porous scaffolds within microfluidic channels

Fernanda Zamboni, Marie Keays, Sheri L. Hayes, Ahmad B. Albadarin, GAVIN WALKER, PATRICK KIELY, MAURICE COLLINS

Accepted Manuscript

Title: Enhanced Cell viability in Hyaluronic Acid Coated Poly(lactic-co-glycolic acid) Porous Scaffolds within Microfluidic Channels

Authors: Fernanda Zamboni, Marie Keays, Sheri Hayes, Ahmad B. Albadarin, Gavin M. Walker, Patrick A. Kiely, Maurice N. Collins

PII: S0378-5173(17)30919-5
DOI: http://dx.doi.org/10.1016/j.ijpharm.2017.09.053
Reference: IJP 17034

To appear in: *International Journal of Pharmaceutics*

Received date: 20-6-2017
Revised date: 17-9-2017
Accepted date: 18-9-2017

Please cite this article as: Zamboni, Fernanda, Keays, Marie, Hayes, Sheri, Albadarin, Ahmad B., Walker, Gavin M., Kiely, Patrick A., Collins, Maurice N., Enhanced Cell viability in Hyaluronic Acid Coated Poly(lactic-co-glycolic acid) Porous Scaffolds within Microfluidic Channels.International Journal of Pharmaceutics http://dx.doi.org/10.1016/j.ijpharm.2017.09.053

Enhanced Cell viability in Hyaluronic Acid Coated Poly(lactic-co-glycolic acid) Porous Scaffolds within Microfluidic Channels

Fernanda Zamboni[1], Marie Keays[1], Sheri Hayes[2], Ahmad B. Albadarin[1], Gavin M. Walker[1], Patrick A. Kiely[1,2]and Maurice N Collins[1*]

[1]Bernal Institute, University of Limerick, Ireland.

[2]Graduate Entry Medical School and Health Research Institute (HRI), University of Limerick, Limerick, Ireland

Corresponding author: maurice.collins@ul.ie tel +353 61202867

Graphical abstract

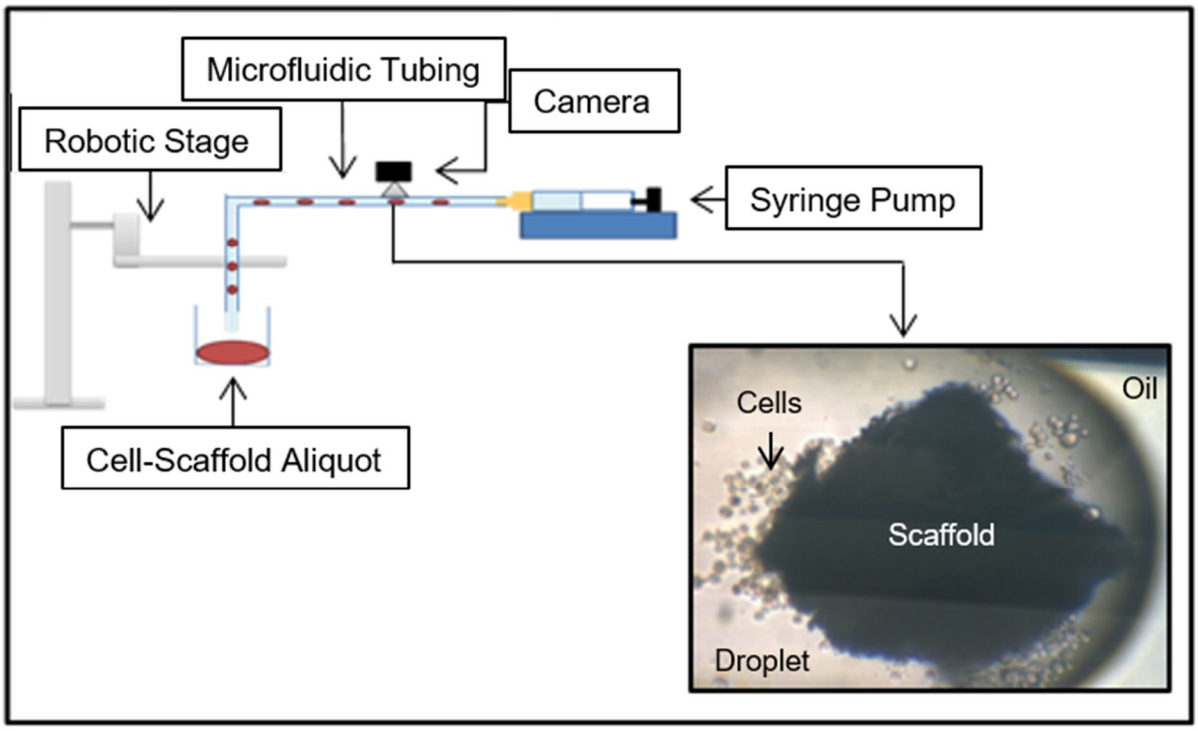

Abstract

The concept of the present work is to produce porous optimised scaffolds of poly(lactic-co-glycolic acid) (PLGA) coated with hyaluronic acid (HA), to provide a suitable microenvironment for cellular proliferation. Freeze dried scaffolds were produced from PLGA with varying lactic acid and glycolic acid ratios along the polymer backbone, as follows: 50:50 ester terminated, 50:50 carboxylate end-group and 85:15 ester terminated. Subsequently, these scaffolds were immersed in crosslinked HA in order for the coating to enhance biological performance. Scaffolds were fully characterized with respect to surface morphology, physical and chemical properties. The biocompatibility of the scaffolds was firstly evaluated using standard L929 fibroblast cells in static culture and subsequently MCF-7 breast cancer cells were seeded on scaffolds which were incorporated within a microfluidic device. The results show that cells were attracted to and adhered to the scaffolds, with a higher affinity for HA coated scaffolds. In our system, cell viability was maintained up to 48h.

Keywords: Scaffolds; PLGA; hyaluronic acid; microfluidics; MCF-7 breast cancer cells

1 Introduction

Cancer is ranked among the leading causes of death around the world, taking second place after cardiovascular disease. In women, specifically, the most prevalent cancer with also the highest mortality rate is breast cancer. An estimate from 2013 depicts that there were 1.8 million new cases of breast cancer and over 464,000 deaths (Fitzmaurice et al., 2015). In order to improve breast cancer outcome and survival rates, early detection still remains the cornerstone of breast cancer control (Hammond et al., 2010; Wolff et al., 2014).

In this scenario, Lab-on-a-Chip devices, such as microfluidics, are emerging as innovative platforms for cancer biology, clinical oncology, and high-throughput drug screening routines (Kang et al., 2014; Rivet et al., 2011; Sabhachandani et al., 2016). The main advantages of microfluidic devices include reduction of costs, increased sensitivity, time-efficiency, reduced reagent and sample volumes, and they also provide unique opportunities for multi-parameter studies on cancer cells, allowing rapid analysis of small amounts of patient derived cells (Mao and Huang, 2012). However, maintaining and expanding cells in droplets of liquid presents challenges as the single cell populations are deficient in adhesion signals. These signals are usually conferred onto cells by the extracellular matrix (ECM) that is a central component of the cells microenvironment and the microenvironment in cancer is known to affect cancer invasion, metastasis and the efficacy of anti-cancer drugs. (Acerbi et al., 2015; Baccelli et al., 2013). It is further recognized that cancer cells respond differently to anti-cancer drugs when maintained under 3-Dimensional (3-D) conditions (Gomes et al., 2015; Lovitt et al., 2015). Therefore, the use of 3-D culture conditions is more physiologically relevant and is better suited to predict the toxicity and efficacy of potential drugs as well as the appropriate expression of biomarkers (Guo et al., 2014; Montanez-Sauri et al., 2015).

Generally, biocompatible and biodegradable synthetic polymers have good mechanical strength (Murphy et al., 2016), but they are relatively hydrophobic (Douglas et al., 2016a; Douglas et al., 2016b) and hinder cell seeding (Souness et al., 2017) due to the lack or absence of cell adhesive motifs such as RGD (Arg-Gly-Asp), REDV (Arg-Glu-Asp-Val) and YIGSR (Tyr–Ile–Gly–Ser–Arg) (Mobasseri et al., 2017). By contrast, naturally-derived ECM polymers offer hydrophilic environments lacking in structural stability, although a number of crosslinking methods have been utilised to increase their structural stability (Collins and Birkinshaw, 2008b). In recent years, a considerable amount of research has been carried out on PLGA because of its promising applications on drug delivery carriers (Lin et al., 2015; Pamujula et al., 2012), cell encapsulation and tissue engineering (Braghirolli et al., 2015; Chang et al., 2013). PLGA is a semi-synthetic polymer with physical properties which are dependent on the ratio of lactide to glycolide, for example poly glycolic acid (PGA) is a highly crystalline material, however the copolymerization with poly lactic acid makes PLGA amorphous, resulting in increased hydration and degradation rates (Makadia and Siegel, 2011).

HA – a non-sulphated glycosaminoglycan – is also being studied for a variety of applications that includes: tissue engineering (Song et al., 2013) wound healing drug delivery systems (Choh et al., 2011), cell encapsulation (Zamboni and Collins, 2017) and microfluidics applications (Burdick and Prestwich, 2011). The structure of HA contains HA contains alternating units of glucuronic acid and glucosamine. This natural polymer is one of the components of the extracellular matrix (ECM) of all connective tissues and exhibits functions related to cell signalling, wound repair (of which cell membrane receptors are involved into directly cell-HA interactions) (Nasreen et al., 2002) and matrix organization. HA is hydrophilic and rapidly degrades *in vivo* by physiological enzymes called hyaluronidases (Stern, 2004) or by hydrolysis (Tamer et al., 2014; Valachova et al., 2015; Valachova et al.,

2016). However, a variety of chemical modifications can be performed in order to increase HA structural stability (Collins and Birkinshaw, 2007) and form hydrogels (Collins and Birkinshaw, 2013a).

Currently, microfluidics research on cancer biology uses cell spheroids (Sabhachandani et al., 2016). However, when cells agglomerate to form a spheroid, the inner core of the cell mass becomes ischemic as a result of decreased inward diffusion of nurturing molecules (Bertuzzi et al., 2010). The possibility of integrating a polymeric scaffold into microfluidic droplets serving as supportive vehicles for cell expansion allows appropriate surface area and porosity for maximum cell adhesion and core viability. In this context, the aim of this study is to generate a platform that will expand cell populations enabling thousands of experiments from a single biopsy. A further objective is to establish an optimised microenvironment for cell adhesion and proliferation for up to 48 hrs within a droplet through the determination of the influence of different PLGA ratios and functionalized end-groups on the scaffold performance within the droplet, as well as the ability of HA to improve cellular performance. While there have been studies on cell carriers within microfluidic devices for cell expansion using hydrogels (Wu et al., 2017) and porous scaffolds of poly-ε-caprolactone have been used as microcarriers in static and agitated cell culture (Li et al., 2017). However, to the authors knowledge, there are have been no reports to date about scaffolds being used within microfluidic channels to support cell culture.

2 Materials and Methods

2.1 Materials

HA, with an average molecular weight (Mw) of 1.44 MDa, was supplied by Contipro Group (Dolni Dobrouc, Czech Republic) as a dry powder. PLGA 50:50 ester terminated (Mw: 51.0

KDa), PLGA 85:15 ester terminated (Mw: 97.6 KDa) and PLGA 50:50 carboxylate terminated (Mw: 43.9 KDa) were purchased from LACTEL manufacturer (Birmingham, AL, USA). L929 fibroblast cell lines and Michigan Cancer Foundation 7 (MCF-7) from human breast adenocarcinoma cell line were purchased from commercial sources. 1-ethyl-3-(3-dimethylamonipropryl)carbodiimide (EDC), L-leucine methylester (LME), Dulbecco's modified Eagle Medium (DMEM), trypsin-EDTA 0.25%, fetal bovine serum (FBS), L-glutamine and antibiotics were purchased from Sigma Aldrich (St. Louis, MO, USA). Alamar Blue cell viability reagent was purchased from Invitrogen (Paisley, UK). PD5 silicon oil was purchased from Momentive. All other reagents used in this work were of analytical grade purchased from Lennox Laboratories Supplies (Dublin, Ireland).

2.2 Fabrication of HA Coated PLGA scaffold:

PLGA was dissolved in 1,4-dioxan under agitation for 48 hours, at 25ºC and 120 RPM, to prepare a PLGA 26 wt% solution. 750 µL of the solution was transferred to a 24 well-plate mould which was followed by freezing at –20ºC for 24 hours. Freeze drying (Eurotherm LS40/60, Severn Science Ltd, Bristol, England) was carried out using the following conditions: cooling for 8 hours at -30ºC, first drying for 12 hours at -5ºC under 0.1-0.5 mbar and secondary drying for 8 hours at 30ºC (under vacuum) to remove dioxane from the PLGA, thus obtaining a disk-shaped scaffold. HA 1wt% solution was prepared with distilled water under oscillation for 24 hours at 25ºC at 120 RPM. Once dissolved, the homogeneous system had the pH adjusted to 4.00 using hydrochloric acid 1M. HA crosslinking was carried out with the addition of EDC and LME (EDC:LME:HA, 1.5:1:1), where the mixture was held at room temperature for 5h to complete the reaction (Collins and Birkinshaw, 2008a; Collins and Birkinshaw 2013b). The HA coating solution was then stirred at 37°C for 1 minute. A dip-coating method was employed to coat the scaffolds with the HA coatings. Scaffolds were immersed in the coating solution for 3 minutes followed by drying for 5 minutes at room

temperature. The coating process was performed two times for each scaffold. Once coated, the scaffolds were allowed to dry at room temperature overnight. The viscosity of the HA solution was low so complete diffusion into the scaffold is expected.

2.3 Scaffold characterization

Morphology of PLGA and PLGA/HA scaffolds were analysed using scanning electron microscopy (SEM). Scaffolds were gold-coated using a sputter coater for 60 seconds at a current of 40 mA. SEM micrographs were obtained using a TM-1000 table top microscope (Hitachi, Japan). Pore size measurements were analysed using a magnification of 200x with ImageJ software. Mechanical compression test of the scaffolds was performed using a Tinius Olsen H20K-W with a crosshead speed of 2 mm/minute at room temperature. The Young's modulus was obtained from the slope of stress vs strain plots where strain < 6% (linear region), in accordance with Hooke's law. Samples were tested in triplicate. All spectra were recorded on a Perkin Elmer spectrum 100 FT-IR spectrometer operating in the Attenuated Total Reflectance (ATR) mode. Each FTIR spectrum was scanned 30 times with a resolution of 2 cm^{-1}. The ranges used were from 4000 - 650 cm^{-1}. DSC analysis was carried out using a Perkin Elmer DSC 6 Pyris Series. The thermal analysis profiles were of freeze dried samples and the temperature was increased from ambient to 350^{o}C at a rate of 10^{o}C/minute under a 20 mL/minute of nitrogen gas flow. 1 µL droplets of distilled water were captured using a KSV contact angle test apparatus with angles calculated using CAM software. 8 measurements were performed per sample.

Swelling of PLGA 26% and PLGA/HA hybrid scaffolds were studied in 2 mL of phosphate buffered saline (pH 7.4) incubated at 37^{o}C in a shaker bath at 100 RPM. Scaffolds were removed at various time intervals; excess solution was wiped and sample weights were recorded. Swelling ratios were calculated as follows:

$$Swelling \quad ratio = \left[\frac{Ws - Wd}{Wd}\right] \times 100$$

where *W*d is the dry weight and *W*s is the weight of the scaffold after the incubation time. All swelling measurements were carried out in triplicate.

2.4 Biological analysis

L929 and MCF-7 cells were cultured in DMEM with 10% FBS, 1% streptomycin-penicillin solution and 2 mM of L-glutamine at 37ºC with 5% CO_2 in a humidified atmosphere. This medium was replenished every 3 days until 80% confluence was reached. Prior to cell seeding, scaffolds were sterilized using UV radiation for 2 hours and then transferred to 24 well-plates.

For the viability study, both cell lineages were quantified by resazurin - Alamar Blue (AB) - metabolic activity assay. Due to AB redox nature, in which the oxidized form of AB (substrate) contained in the medium is reduced (product) by the various components of the cellular respiration chain, (when cells are dead, they lose the ability to convert the substrate into product), the reduced form of AB is proportional to the number of viable cells present in the different planes of a 3-D microenvironment, being able to provide a quantitative analysis of cell viability and assuming that the metabolic activity maintains constant throughout the testing conditions, quantification of cell proliferation is also possible. For the static culture of fibroblasts, cells were seeded onto uncoated-PLGA scaffolds, HA-coated PLGA scaffolds and the well (control group) of a 24 well-plate at a concentration of 50.000 cells/mL (n=3). After an initial 4 hours of incubation to allow cell attachment, scaffolds were transferred to a new well plate. This was made necessary in order to exclude the influence of any unadhered cells in medium suspension or cells adhered to the surface of the well. Then, AB was added to the media at a concentration of 10% as specified by the manufacturer. The well plates were returned to the incubator and aliquots of the media were taken at 4 hours, 24 hours and 48

hours of incubation to provide a continuous monitoring of cell culture over time. Aliquots were measured in a 96 well-plate and fluorescence readings were performed at 540 nm and 590 nm. For the microfluidic culture, droplets were collected into 96 well-plates at specific times.

For cell attachment analysis, L929 cells were seeded onto HA-coated PLGA 85:15 ester terminated scaffolds for 48 hours and then cells were live stained with the molecular probe (Hoechst 33342) as described by the manufacturer (Life Technologies). Cell fluorescence imaging was captured by the software CellSens using an Olympus IX83 microscope.

2.5 Microfluidics

A microfluidic device was used to create miniaturised culture droplets. A syringe pump under negative pressure was used to create a flow through a PTFE tubing of 812 μm diameter. The tubing was immersed into the aqueous sample containing the cells-scaffold mixture and pulled back out of the sample to the oil phase using a robotic stage. This action creates the droplets and is continuously carried out at set intervals to consistently create equidistant droplets. Once the droplets are created they were monitored through the tubing using an Olympus CK×31 microscope and an Image Source CCD camera (Fig1). The droplets were then incubated at 37ºC in 5% CO_2 and monitored over 24 hours. Scaffolds were reduced to sizes less than 800 μm and added to a suspension of MCF-7 containing 1×10^6 cells/mL. Droplets of around 600 nL were formed inside the circular PTFE microfluidic channel. The droplets were encapsulated in PD5 silicon oil which creates a barrier layer around the droplet to prevent it from attaching to the wall of the microfluidic tubing.

2.6 Statistical Analysis

Data are presented as mean ± standard deviation (s.d.) and analysed using ANOVA followed by Student's T test, for repeated measurement design. *p-value* < 0.05 (*) was considered to be significant.

3 Results and Discussion

Scaffolds of three different PLGA copolymers were produced by freeze drying and the dimensions of the final scaffolds are shown in table 1. The surface morphology of the scaffolds was assessed using SEM (Fig 2) and the images showed that there are differences between the copolymer ratios. PLGA 50:50 exhibited a surface skin type structure with smaller number of pores with larger sizes [PLGA 50:50 ester terminated have an average pore size of 726.56 μm^2 (±649.49) and PLGA 50:50 carboxylate end-group have an average pore size of 801.602 μm^2 (±272.37)], which was previously reported by Ho et al (2004) (Ho et al., 2004), while PLGA 85:15 showed no surface skin and a larger number of smaller pores [average pore size of 229.22 μm^2(±63.66)]. It can also be seen that interconnected small pores appear inside the scaffolds which is ideal for cell growth and proliferation.

By applying a compressive load, stress vs strain values were obtained (supplementary data) for each group of scaffolds and when strain was smaller than 6% (linear region defined by Hooke's law), the Young's moduli (YM) were calculated and results are presented as mean (± s.d.). PLGA 50:50 ester terminated scaffolds had YM of 4.34 MPa (±0.284), PLGA 50:50 carboxylate end-group had YM of 3.35 MPa (±1,21) and PLGA 85:15 ester terminated had YM of 5.48 MPa (±0,80). These values are comparable to the those of cartilage, of which their mechanical properties lies between hard tissue (bone and teeth) and soft tissue (skin, muscles, fat) (Duck, 1990).

For the chemical analysis of HA-coated PLGA scaffolds (Fig3a), characteristic HA bands can be distinguished, indicating that PLGA scaffolds were successfully coated with HA. Firstly, a broad band centred at 3400 cm^{-1} was assigned to hydrogen bonded O–H stretching vibrations, secondly, a region of C=O stretching vibrations and secondary amide (NH) ranging 1800–1500 cm^{-1} and thirdly, a region for C-C stretching vibrations of the pyranoid ring and C–O–C stretching vibration of glycosidic bonds from 1200–950 cm^{-1}, as previouly reported in Gomez-Ordonez et al., 2011 (Gomez-Ordonez and Ruperez, 2011). The analysis of the FT-IR spectra regarding the PLGA, can show the presence of a band centred at 1735 cm^{-1} assigned to C=O stretching vibrations for carbonyl groups, either of carboxylic acids or esters. The band for the carboxylate anion form (COO^-) at 1600 cm^{-1} was analysed in order to verify if the carboxylate end group of PLGA 50:50 was hydrated. With the absence of the COO^- band, it is assumed that the hydrated form is present. This is confirmed by the appearance of bands related to C–OH deformation vibration with contribution of O–C–O symmetric stretching vibration of carboxylic group at 1450-1400 cm^{-1}, as previouly reported in Erebetta et al., 2012 (Erbetta, 2012).

PLGA is an amorphous copolymer of crystalline polyglycolic acid (PGA) and amorphous poly-D-L-lactic acid (PDLLA). Due to PLGA's amorphous structure, it displays a glass transition temperature (Tg) but not a melting transition temperature (Tm) before chemical degradation. PLGA is described to have a Tg above 37 °C, however this depends on the lactide to glycolide ratios. DSC results (Fig3b) show that PLGA 85:15 ratio has the highest glass transition temperature (54.74 ^oC), when compared to both PLGA 50:50 ratios, due to higher lactide content similar results were reported in Erebetta et al., 2012 and Manoochehri et al. 2013 (Erbetta, 2012; Manoochehri et al., 2013). It also shows that PLGA 50:50 ester

terminated group shows a higher Tg (52.48 ^{o}C) when compared with the PLGA 50:50 carboxylate end group (50.82 ^{o}C), due to differences between the end groups which has been confirmed by Gentile et al., 2014 (Gentile et al., 2014).

The higher Tg values presented by all PLGA groups in comparison to the average 37 °C can also be attributed to the lyophilization process. It has been previously reported that water acts as a plasticizer in PLGA, thus decreasing Tg below 37 °C which displays a rubbery state. However after freeze drying, when water is removed, Tg increases above 37 °C, thus indicating that the polymer is in a glassy state (Faisant et al., 2002), which is in agreement with the results shown above.

Figures 4 and 5 illustrate the effect of HA on PLGA surfaces. They show that PLGA contact angles have been significantly reduced ($p<0.01$) when coated with HA, thereby increasing the hydrophilicity of the entire structure. As a result, HA-coated PLGA scaffolds have higher water uptakes than uncoated-PLGA scaffolds. The general tendency is for the HA-coatings on the PLGA scaffolds swell to their equilibrium water content which is followed by subsequent degradation via chain scission associated with hydrolysis. Taking the scaffold materials itself, bulk erosion degradation occurs as result of hydrolysis, while uncoated-PLGA scaffolds are hydrolytically more stable as the HA coating attracts and retains moisture. It is well established that crosslinking decreases HA degradation rates, which is observed after 72 hours of incubation but withstands for the whole period of analysis (supplementary data).

From the swelling index profiles (Figure 6) it can be observed that scaffolds of PLGA 50:50 carboxylate end-groups were fully degraded at 21 days, demonstrating faster degradation rates associated with hydrophilic carboxylates as opposed to ester end-capped biopolymers (Gentile et al., 2014). Degradation rates are also influenced by parameters such as the molecular weight and the degree of crystallinity; the latter being closely associated to the

ratio of monomers in the copolymer. The glycolide component decreases the degree of crystallinity of the copolymer and as a result increases hydration and hydrolysis rates (Miller et al., 1977; You et al., 2005) while the lactide methyl side groups make it more hydrophobic than the glycolide side groups therefore decreasing degradation rates (Makadia and Siegel, 2011). For these reasons, the swelling index profile for PLGA 85:15 ester terminated shows the slowest degradation rate, because it has higher Mw and Tg than the other two copolymers. Overall, the results demonstrate the stability of the scaffolds and their suitability for this application.

Fibroblasts (L929 cells) were used to optimise scaffold selection for the microfluidic device. Biocompatibility of the scaffold was assessed by culturing cells on the scaffold and measuring the metabolic activity after incubation of the cells with the scaffold (Fig7a). Cell viability and proliferation results show that HA-coated PLGA 85:15 ester terminated scaffolds offer better microenvironments for cell survival in comparison to other HA-coated PLGA scaffolds at all time points ($p<0.001$). It is envisioned that the surface morphology of the scaffold has a possible influence on the viability results, showing that the HA-coated PLGA 85:15 ester terminated scaffolds which provide a larger number of pores (Fig1c) also have the better viability results. The live staining images of the cells (Fig7b) show that cells are attached to the surface of the scaffold. It is postulated that cells are localized within the pores, but further investigation should be carried out to confirm cell infiltration within the scaffolds. The morphology of the PLGA scaffold seems to have a stronger influence on cell attachment and viability, because for the PLGA 50:50 scaffolds, both ester and carboxylate terminated show the same surface morphology and similar cell viability, especially at 24h ($p>0.05$). HA-coated PLGA 85:15 ester terminated scaffolds showed superior results, such as increased porosity, slower degradation rate and higher cell viability values ($p<0.001$) when

compared to other PLGA groups. Therefore, HA-coated PLGA 85:15 ester terminated scaffolds were chosen to carry out a trial on breast cancer cells (MCF-7 cells) within microfluidic droplets.

For droplets containing MCF-7 cells and scaffolds, it was noticeable that scaffolds tend to attract and attach cells to their surface within 24 hours of incubation as shown in Figure 1. It is presumed that HA contributes to the attraction of cells to the surface of the scaffold by specific cell-HA receptors being directly involved in adhesion and migration responses, such as CD44 and RHAMM (Acharya et al., 2008). After 4 hours, 24 hours and 48 hours of incubation, droplets containing the scaffolds were transferred to 96 well-plates and washed with PBS in order to analyse cell viability. As it can be seen in Figure 8, cells maintain viability and increase proliferation up to 48h within the microfluidic device. This result demonstrates that is possible to use these scaffolds as a microenvironment for cell adhesion and proliferation within microfluidics droplets.

4 Conclusion:

Scaffolds of three different PLGA copolymers were successfully produced by freeze drying. These scaffolds were coated with crosslinked HA to improve their hydrophilicity and biological performance. L929 fibroblast cells were used to assess the biocompatibility. Results showed that HA-coated PLGA 85:15 ester terminated scaffolds maintained higher viability values in comparison to other scaffolds in this study. This finding can be attributed to the differences in the surface morphology of the scaffolds. After, MCF-7 breast cancer cells were used in order to verify the possibility of using these scaffolds as cell carriers within a microfluidic device, with the goal of providing solutions for the expansion of cells within droplets in order to realise the ambition of being able to execute thousands of experiments with a single biopsy. Overall, these findings demonstrate the first step towards more complex

studies on cancer biology and biomarkers expression which will be crucial for post-diagnosis and future individualised drug screening for personalised breast cancer treatment and diagnosis.

5 Acknowledgements:

We would like to acknowledge the financial support from the Irish Research Council (IRC) grant number GOIPG/2015/3577 (to FZ) and Science Foundation Ireland grant 13/CDA/2228 (to PK). All authors declare that they have no conflict of interests.

6 References

Acerbi, I., Cassereau, L., Dean, I., Shi, Q., Au, A., Park, C., Chen, Y.Y., Liphardt, J., Hwang, E.S., Weaver, V.M., 2015. Human breast cancer invasion and aggression correlates with ECM stiffening and immune cell infiltration. Integr Biol-Uk 7, 1120-1134.

Acharya, P.S., Majumdar, S., Jacob, M., Hayden, J., Mrass, P., Weninger, W., Assoian, R.K., Pure, E., 2008. Fibroblast migration is mediated by CD44-dependent TGF beta activation. Journal of cell science 121, 1393-1402.

Baccelli, I., Schneeweiss, A., Riethdorf, S., Stenzinger, A., Schillert, A., Vogel, V., Klein, C., Saini, M., Bauerle, T., Wallwiener, M., Holland-Letz, T., Hofner, T., Sprick, M., Scharpff, M., Marme, F., Sinn, H.P., Pantel, K., Weichert, W., Trumpp, A., 2013. Identification of a population of blood circulating tumor cells from breast cancer patients that initiates metastasis in a xenograft assay. Nat Biotechnol 31, 539-U143.

Barbanti, S.H.Z., C. A. C.; Duek, E. A. R., 2005. Bioresorbable Polymers in Tissue Engineering. Polimeros: Ciencia e Tecnologia 15, 13-25.

Bertuzzi, A., Fasano, A., Gandolfi, A., Sinisgalli, C., 2010. Necrotic core in EMT6/Ro tumour spheroids: Is it caused by an ATP deficit? J Theor Biol 262, 142-150.

Blehm, B.H., Jiang, N., Kotobuki, Y., Tanner, K., 2015. Deconstructing the role of the ECM microenvironment on drug efficacy targeting MAPK signaling in a pre-clinical platform for cutaneous melanoma. Biomaterials 56, 129-139.

Braghirolli, D.I., Zamboni, F., Acasigua, G.A., Pranke, P., 2015. Association of electrospinning with electrospraying: a strategy to produce 3D scaffolds with incorporated stem cells for use in tissue engineering. International journal of nanomedicine 10, 5159-5169.

Burdick, J.A., Prestwich, G.D., 2011. Hyaluronic acid hydrogels for biomedical applications. Advanced materials 23, H41-56.

Chang, N.J., Jhung, Y.R., Yao, C.K., Yeh, M.L., 2013. Hydrophilic gelatin and hyaluronic acid-treated PLGA scaffolds for cartilage tissue engineering. Journal of applied biomaterials & functional materials 11, e45-52.

Choh, S.Y., Cross, D., Wang, C., 2011. Facile synthesis and characterization of disulfide-cross-linked hyaluronic acid hydrogels for protein delivery and cell encapsulation. Biomacromolecules 12, 1126-1136.

Collins, M.N., Birkinshaw, C., 2007. Comparison of the effectiveness of four different crosslinking agents with hyaluronic acid hydrogel films for tisslue-culture applications. Journal of Applied Polymer Science 104, 3183-3191.

Collins, M.N., Birkinshaw, C., 2008a. Investigation of the swelling behavior of crosslinked hyaluronic acid films and hydrogels produced using homogeneous reactions. Journal of Applied Polymer Science 109, 923-931.

Collins, M.N., Birkinshaw, C., 2008b. Physical properties of crosslinked hyaluronic acid hydrogels. J Mater Sci-Mater M 19, 3335-3343.

Collins, M.N., Birkinshaw, C., 2013a. Hyaluronic acid based scaffolds for tissue engineering-A review. Carbohydrate polymers 92, 1262-1279.

Collins, M.N., Birkinshaw, C., 2013b. Hyaluronic Acid Solutions – A processing method for Chemical Modification Journal of Applied Polymer Science**,** vol 130, issue 1, pgs 145-152.

Douglas, P,. Kuhs, M., Sajjia, M.. Khraisheh, M., Walker, G., Collins M.N. and Albadarin A.B. 2016a. “Bioactive PCL matrices with a range of structural & rheological properties”, Reactive and Functional Polymers, Vol 101, 54-62.

Douglas, P., Albadarin, A.B., Sajjia, M., Mangwandi, C., Kuhs, M., Collins, M.N. and Walker G.M. 2016b. “Effect of poly ethylene glycol on the mechanical and thermal properties of bioactive Poly (ε–caprolactone) melt extrudates for pharmaceutical applications”, International Journal of Pharmaceutics, Vol 500, 179-186.

Duck, F.A., 1990. Chapter 5 - Mechanical Properties of Tissue, in: Duck, F.A. (Ed.), Physical Properties of Tissues. Academic Press, London, pp. 137-165.
Erbetta, C.D.C.A., R. J.; Resende, J. M.; Freitas, R. F. S.; Sousa, R. G., 2012. Synthesis and Characterization of Poly(D,L-Lactide-co-Glycolide) Copolymer. journal of Biomaterials and Nanobiotechnology 3, 18.
Esserman, L.J., Joe, B.N., Breast biopsy, in: Chagpar, A., Chen, W. (Eds.). UpToDate, UpToDate.
Faisant, N., Siepmann, J., Benoit, J.P., 2002. PLGA-based microparticles: elucidation of mechanisms and a new, simple mathematical model quantifying drug release. Eur J Pharm Sci 15, 355-366.
Fitzmaurice, C., Dicker, D., Pain, A., Hamavid, H., Moradi-Lakeh, M., MacIntyre, M.F., Allen, C., Hansen, G., Woodbrook, R., Wolfe, C., Hamadeh, R.R., Moore, A., Werdecker, A., Gessner, B.D., Te Ao, B., McMahon, B., Karimkhani, C., Yu, C., Cooke, G.S., Schwebel, D.C., Carpenter, D.O., Pereira, D.M., Nash, D., Kazi, D.S., De Leo, D., Plass, D., Ukwaja, K.N., Thurston, G.D., Yun Jin, K., Simard, E.P., Mills, E., Park, E.K., Catala-Lopez, F., deVeber, G., Gotay, C., Khan, G., Hosgood, H.D., 3rd, Santos, I.S., Leasher, J.L., Singh, J., Leigh, J., Jonas, J.B., Sanabria, J., Beardsley, J., Jacobsen, K.H., Takahashi, K., Franklin, R.C., Ronfani, L., Montico, M., Naldi, L., Tonelli, M., Geleijnse, J., Petzold, M., Shrime, M.G., Younis, M., Yonemoto, N., Breitborde, N., Yip, P., Pourmalek, F., Lotufo, P.A., Esteghamati, A., Hankey, G.J., Ali, R., Lunevicius, R., Malekzadeh, R., Dellavalle, R., Weintraub, R., Lucas, R., Hay, R., Rojas-Rueda, D., Westerman, R., Sepanlou, S.G., Nolte, S., Patten, S., Weichenthal, S., Abera, S.F., Fereshtehnejad, S.M., Shiue, I., Driscoll, T., Vasankari, T., Alsharif, U., Rahimi-Movaghar, V., Vlassov, V.V., Marcenes, W.S., Mekonnen, W., Melaku, Y.A., Yano, Y., Artaman, A., Campos, I., MacLachlan, J., Mueller, U., Kim, D., Trillini, M., Eshrati, B., Williams, H.C., Shibuya, K., Dandona, R., Murthy, K., Cowie, B., Amare, A.T., Antonio, C.A., Castaneda-Orjuela, C., van Gool, C.H., Violante, F., Oh, I.H., Deribe, K., Soreide, K., Knibbs, L., Kereselidze, M., Green, M., Cardenas, R., Roy, N., Tillmann, T., Li, Y., Krueger, H., Monasta, L., Dey, S., Sheikhbahaei, S., Hafezi-Nejad, N., Kumar, G.A., Sreeramareddy, C.T., Dandona, L., Wang, H., Vollset, S.E., Mokdad, A., Salomon, J.A., Lozano, R., Vos, T., Forouzanfar, M., Lopez, A., Murray, C., Naghavi, M., 2015. The Global Burden of Cancer 2013. JAMA Oncol 1, 505-527.
Gentile, P., Chiono, V., Carmagnola, I., Hatton, P.V., 2014. An overview of poly(lactic-co-glycolic) acid (PLGA)-based biomaterials for bone tissue engineering. International journal of molecular sciences 15, 3640-3659.
Gomes, L.R., Vessoni, A.T., Menck, C.F., 2015. Three-dimensional microenvironment confers enhanced sensitivity to doxorubicin by reducing p53-dependent induction of autophagy. Oncogene 34, 5329-5340.
Gomez-Ordonez, E., Ruperez, P., 2011. FTIR-ATR spectroscopy as a tool for polysaccharide identification in edible brown and red seaweeds. Food Hydrocolloid 25, 1514-1520.
Guo, W.M., Loh, X.J., Tan, E.Y., Loo, J.S., Ho, V.H., 2014. Development of a magnetic 3D spheroid platform with potential application for high-throughput drug screening. Mol Pharm 11, 2182-2189.
Hammond, M.E., Hayes, D.F., Dowsett, M., Allred, D.C., Hagerty, K.L., Badve, S., Fitzgibbons, P.L., Francis, G., Goldstein, N.S., Hayes, M., Hicks, D.G., Lester, S., Love, R., Mangu, P.B., McShane, L., Miller, K., Osborne, C.K., Paik, S., Perlmutter, J., Rhodes, A., Sasano, H., Schwartz, J.N., Sweep, F.C., Taube, S., Torlakovic, E.E., Valenstein, P., Viale, G., Visscher, D., Wheeler, T., Williams, R.B., Wittliff, J.L., Wolff, A.C., 2010. American Society of Clinical Oncology/College Of American Pathologists guideline recommendations for immunohistochemical testing of estrogen and progesterone receptors in breast cancer.

Journal of clinical oncology : official journal of the American Society of Clinical Oncology 28, 2784-2795.
Ho, M.H., Kuo, P.Y., Hsieh, H.J., Hsien, T.Y., Hou, L.T., Lai, J.Y., Wang, D.M., 2004. Preparation of porous scaffolds by using freeze-extraction and freeze-gelation methods. Biomaterials 25, 129-138.
Holle, A.W., Young, J.L., Spatz, J.P., 2016. In vitro cancer cell-ECM interactions inform in vivo cancer treatment. Advanced drug delivery reviews 97, 270-279.
Holohan, C., Van Schaeybroeck, S., Longley, D.B., Johnston, P.G., 2013. Cancer drug resistance: an evolving paradigm. Nat Rev Cancer 13, 714-726.
Kang, D.K., Ali, M.M., Zhang, K.X., Pone, E.J., Zhao, W.A., 2014. Droplet microfluidics for single-molecule and single-cell analysis in cancer research, diagnosis and therapy. Trac-Trend Anal Chem 58, 145-153.
Li, J., Lam, A.T., Toh, J.P., Reuveny, S., Oh, S.K., Birch, W.R., 2017. Tunable Volumetric Density and Porous Structure of Spherical Poly-epsilon-caprolactone Microcarriers, as Applied in Human Mesenchymal Stem Cell Expansion. Langmuir 33, 3068-3079.
Lin, L., Gao, H., Dong, Y., 2015. Bone regeneration using a freeze-dried 3D gradient-structured scaffold incorporating OIC-A006-loaded PLGA microspheres based on beta-TCP/PLGA. Journal of materials science. Materials in medicine 26, 5327.
Lovitt, C.J., Shelper, T.B., Avery, V.M., 2015. Evaluation of chemotherapeutics in a three-dimensional breast cancer model. J Cancer Res Clin Oncol 141, 951-959.
Makadia, H.K., Siegel, S.J., 2011. Poly Lactic-co-Glycolic Acid (PLGA) as Biodegradable Controlled Drug Delivery Carrier. Polymers 3, 1377-1397.
Manoochehri, S., Darvishi, B., Kamalinia, G., Amini, M., Fallah, M., Ostad, S.N., Atyabi, F., Dinarvand, R., 2013. Surface modification of PLGA nanoparticles via human serum albumin conjugation for controlled delivery of docetaxel. Daru : journal of Faculty of Pharmacy, Tehran University of Medical Sciences 21, 58.
Mao, X., Huang, T.J., 2012. Microfluidic diagnostics for the developing world. Lab Chip 12, 1412-1416.
Miller, R.A., Brady, J.M., Cutright, D.E., 1977. Degradation Rates of Oral Resorbable Implants (Polylactates and Polyglycolates) - Rate Modification with Changes in Pla-Pga Copolymer Ratios. J Biomed Mater Res 11, 711-719.
Mobasseri, R., Tian, L.L., Soleimani, M., Ramakrishna, S., Naderi-Manesh, H., 2017. Bio-active molecules modified surfaces enhanced mesenchymal stem cell adhesion and proliferation. Biochem Bioph Res Co 483, 312-317.
Montanez-Sauri, S.I., Beebe, D.J., Sung, K.E., 2015. Microscale screening systems for 3D cellular microenvironments: platforms, advances, and challenges. Cell Mol Life Sci 72, 237-249.
Murphy C.A. and Collins MN. (2016) Microcrystalline cellulose reinforced PLA biocomposite filaments for 3D printing, Polymer Composites, DOI: 10.1002/pc.24069
Nasreen, N., Mohammed, K.A., Hardwick, J., Van Horn, R.D., Sanders, K., Kathuria, H., Loghmani, F., Antony, V.B., 2002. Low molecular weight hyaluronan induces malignant mesothelioma cell (MMC) proliferation and haptotaxis: role of CD44 receptor in MMC proliferation and haptotaxis. Oncology research 13, 71-78.
Pamujula, S., Hazari, S., Bolden, G., Graves, R.A., Chinta, D.D., Dash, S., Kishore, V., Mandal, T.K., 2012. Cellular delivery of PEGylated PLGA nanoparticles. The Journal of pharmacy and pharmacology 64, 61-67.
Rivet, C., Lee, H., Hirsch, A., Hamilton, S., Lu, H., 2011. Microfluidics for medical diagnostics and biosensors. Chem Eng Sci 66, 1490-1507.

Sabhachandani, P., Motwani, V., Cohen, N., Sarkar, S., Torchilin, V., Konry, T., 2016. Generation and functional assessment of 3D multicellular spheroids in droplet based microfluidics platform. Lab Chip 16, 497-505.
Song, J.E., Kim, M.J., Yoon, H., Yoo, H., Lee, Y.J., Kim, H.N., Lee, D., Yuk, S.H., Khang, G., 2013. Effect of hyaluronic acid (HA) in a HA/PLGA scaffold on annulus fibrosus regeneration: In vivo tests. Macromolecular Research 21, 1075-1082.
Souness, A., Zamboni, F., Walker, G.M., Collins, M.N., 2017. Influence of scaffold design on 3D printed cell constructs. Journal of biomedical materials research. Part B, Applied biomaterials.
Stern, R., 2004. Hyaluronan catabolism: a new metabolic pathway. Eur J Cell Biol 83, 317-325.
Tamer, M., Valachová, K., Šoltés, L., 2014. Inhibition of free radical degradation in medical grade hyaluronic acid, in: Collins, M.N. (Ed.), Hyaluronic acid for Biomedical and Pharmaceutical Applications. Smithers Rapra.
Valachova, K., Banasova, M., Topol'ska, D., Sasinkova, V., Juranek, I., Collins, M.N., Soltes, L., 2015. Influence of tiopronin, captopril and levamisole therapeutics on the oxidative degradation of hyaluronan. Carbohydrate polymers 134, 516-523.
Valachova, K., Topol'ska, D., Mendichi, R., Collins, M.N., Sasinkova, V., Soltes, L., 2016. Hydrogen peroxide generation by the Weissberger biogenic oxidative system during hyaluronan degradation. Carbohydrate polymers 148, 189-193.
von Burkersroda, F., Schedl, L., Gopferich, A., 2002. Why degradable polymers undergo surface erosion or bulk erosion. Biomaterials 23, 4221-4231.
Wolff, A.C., Hammond, M.E., Hicks, D.G., Dowsett, M., McShane, L.M., Allison, K.H., Allred, D.C., Bartlett, J.M., Bilous, M., Fitzgibbons, P., Hanna, W., Jenkins, R.B., Mangu, P.B., Paik, S., Perez, E.A., Press, M.F., Spears, P.A., Vance, G.H., Viale, G., Hayes, D.F., American Society of Clinical, O., College of American, P., 2014. Recommendations for human epidermal growth factor receptor 2 testing in breast cancer: American Society of Clinical Oncology/College of American Pathologists clinical practice guideline update. Arch Pathol Lab Med 138, 241-256.
You, Y., Min, B.M., Lee, S.J., Lee, T.S., Park, W.H., 2005. In vitro degradation behavior of electrospun polyglycolide, polylactide, and poly(lactide-co-glycolide). Journal of Applied Polymer Science 95, 193-200.
Wu, J., Chen, Q.S., Liu, W., He, Z.Y., Lin, J.M., 2017. Recent advances in microfluidic 3D cellular scaffolds for drug assays. Trac-Trend Anal Chem 87, 19-31.

Zamboni, F., Collins, M.N., 2017. Cell based therapeutics in type 1 diabetes mellitus. International journal of pharmaceutics 521, 346-356.

Appendix

Tables

Table1 PLGA property values after freeze drying

Copolymer	Functionalized end group	Mw (KDa)	Tg (^{o}C)	Degradation rate	Scaffold dimension (mm)	Pore size (μm^2)	Young's Modulus (MPa)
50:50	ester	51.0	52.48	intermediate	W= 12.93 (±0.284) L= 3.26 (±0.361)	726.56 (±649.49)	4.34 (±0.284)
50:50	carboxylate	43.9	50.82	fast	W= 12.67 (±0.199) L= 2.96 (±0.344)	801.602 (±272.37)	3.35 (±1,21)
85:15	ester	97.6	54.72	slow	W= 13.29 (±0.115) L= 3.71 (±0.248)	229.222 (±63.66)	5.48 (±0,80)

Data are presented as mean (± s.d.). All measurements were analysed in triplicated. Abbreviations: width (W), height (L)

Figures

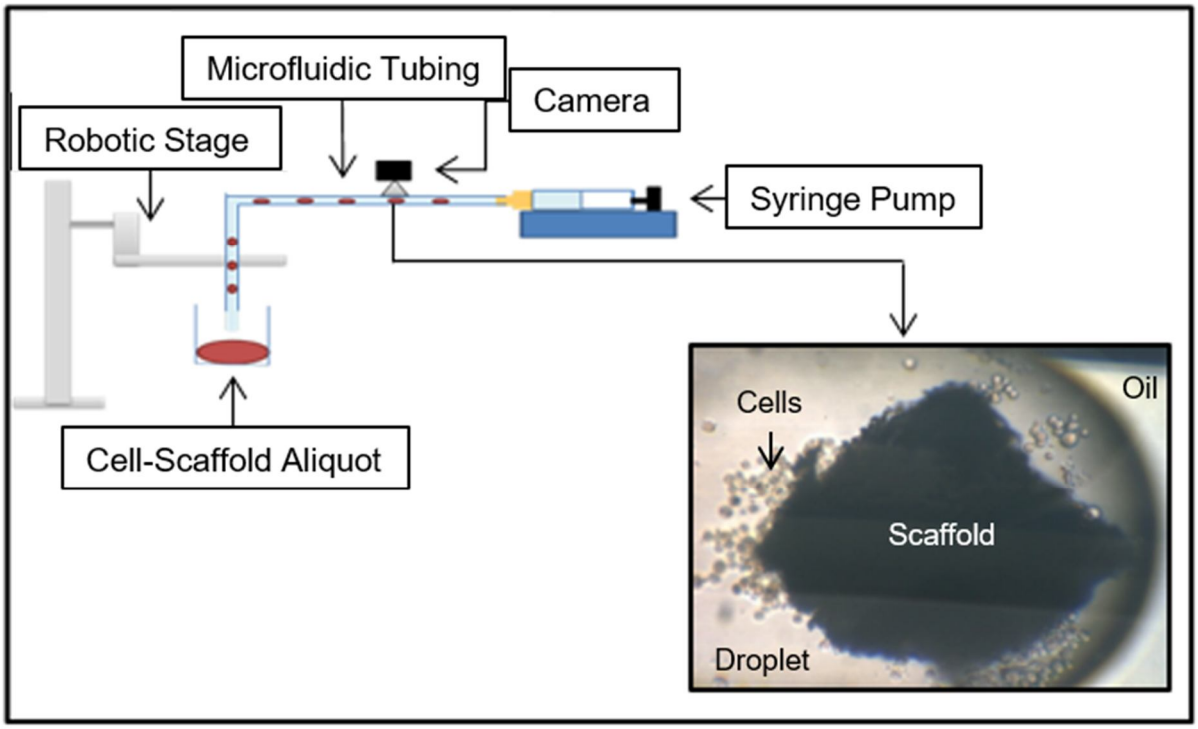

Figure 1: Microfluidics setup and droplet representation

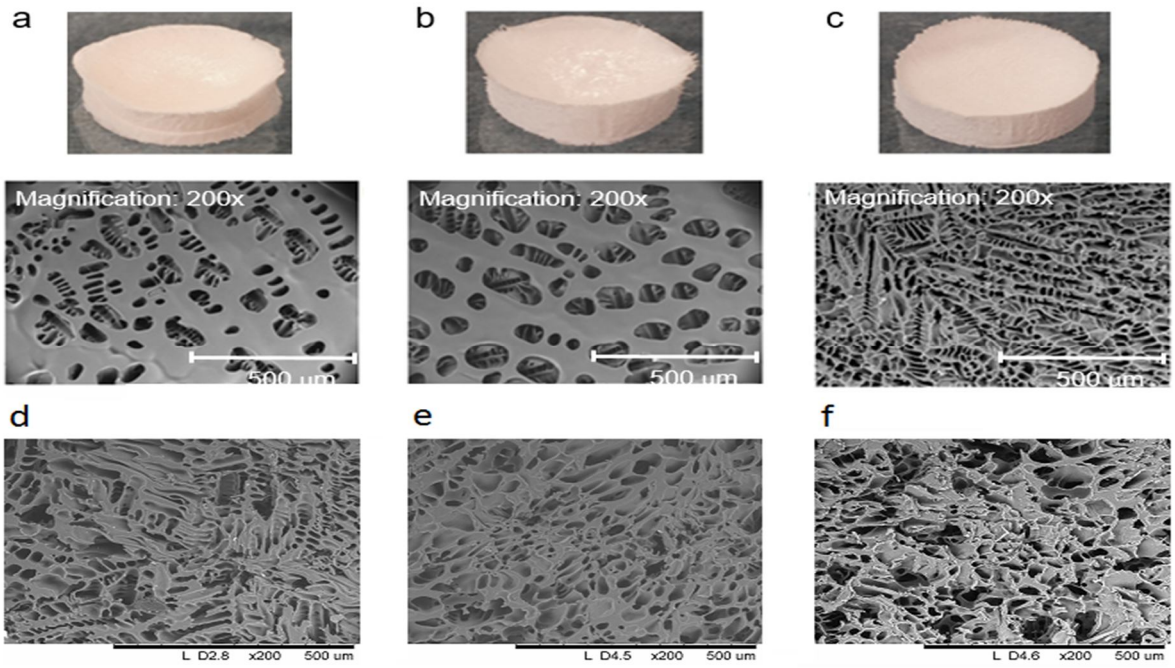

Figure 2: Representative SEM micrographs of the surface (a, b and c) and the cross section (d, e and f) of PLGA 50:50 ester terminated, PLGA 50:50 carboxylate end-group and PLGA 85:15 ester terminated, respectively, after freeze drying.

a)

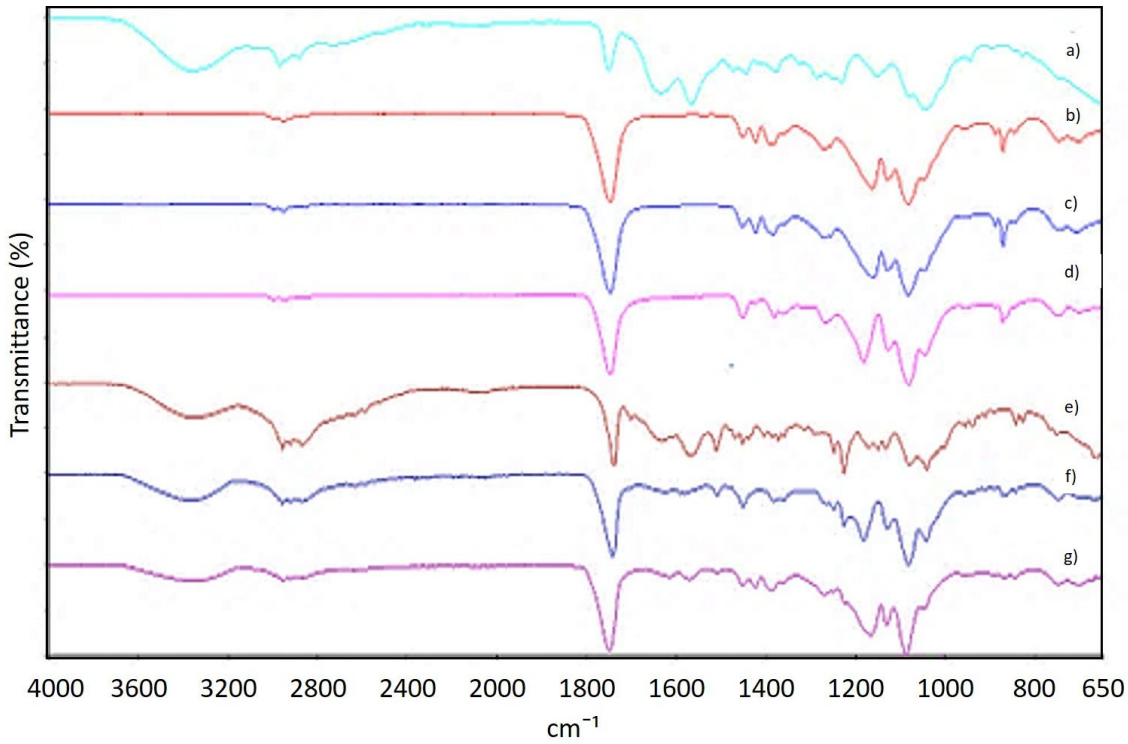

b)

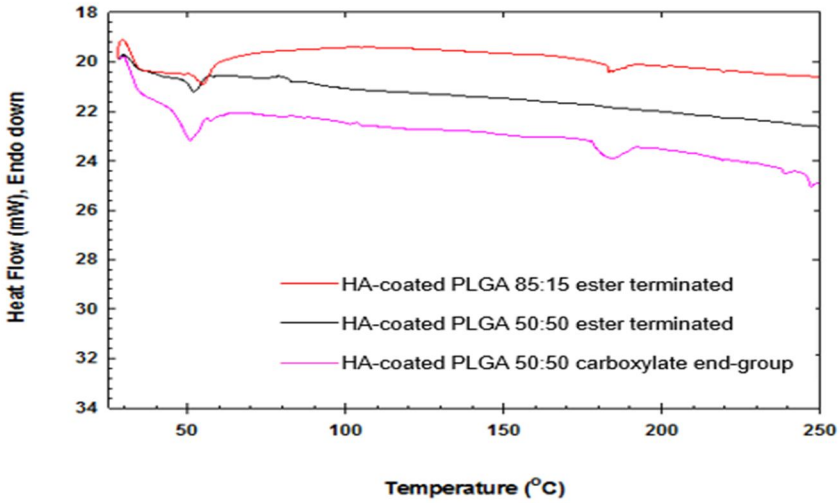

Figure 3: Chemical and thermal evaluation of HA-coated PLGA scaffolds. a) FT-IR spectra of HA (a), uncoated PLGA 85:15 ester terminated (b), uncoated PLGA 50:50 ester terminated (c), uncoated PLGA 50:50 carboxylate end-group (d), HA-coated PLGA 85:15 ester terminated (e), HA-coated PLGA 50:50 ester terminated (f) and HA-coated PLGA 50:50 carboxylate end-group (g). b) DSC curves of HA-coated PLGA 85:15 ester terminated (red), HA-coated PLGA 50:50 ester terminated (black) and HA-coated PLGA 50:50 carboxylate end-group (pink) scaffolds.

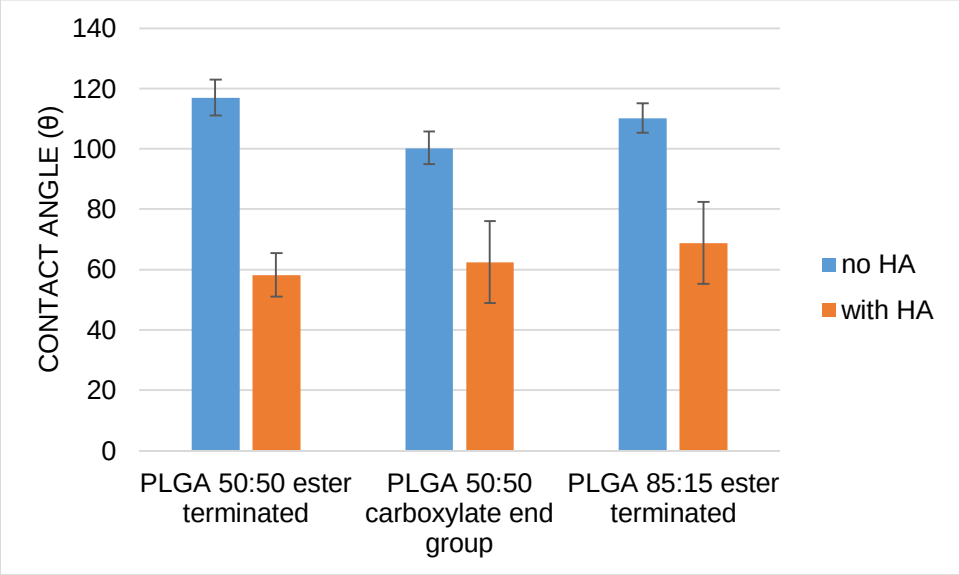

Figure 4: Contact angle for PLGA scaffolds and PLGA/HA hybrid scaffolds. Data are presented as mean (± s.d.). Statistical difference between PLGA and PLGA/HA hybrid groups ($p<0.01$) according to ANOVA followed by Student T test.

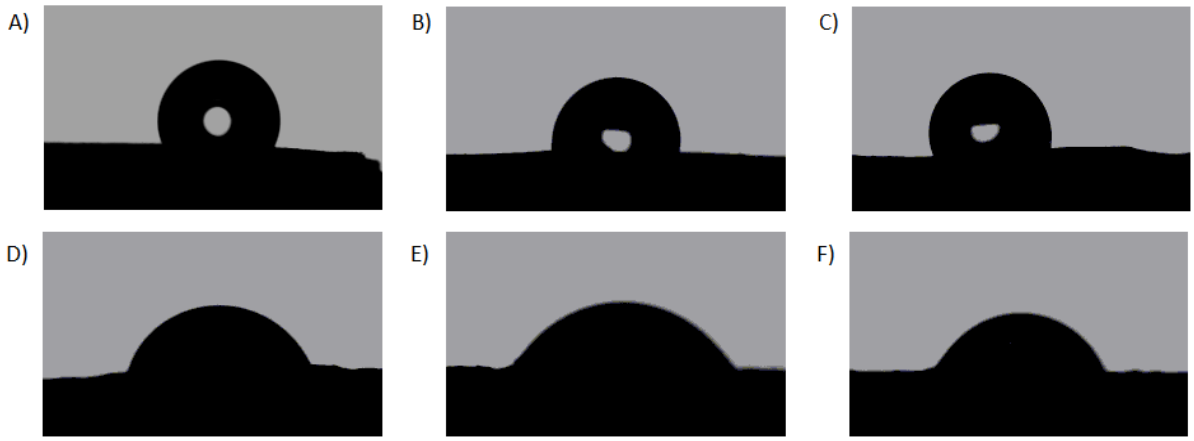

Figure 5: Contact angle representative images. A) PLGA 50:50 ester terminated without HA; B) PLGA 50:50 carboxylate end group without HA; C) PLGA 85:15 ester terminated without HA; D) PLGA 50:50 ester terminated with HA; E) PLGA 50:50 carboxylate end group with HA; F) PLGA 85:15 ester terminated with HA.

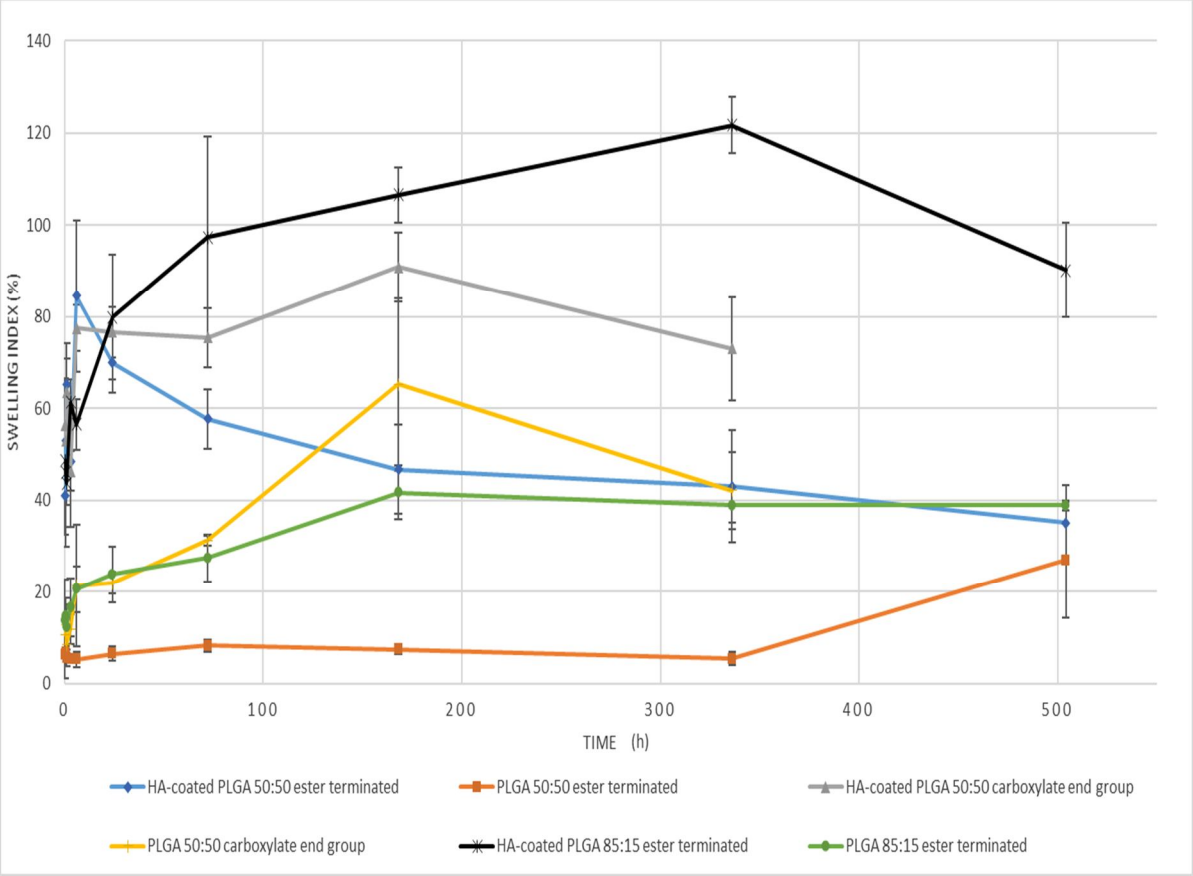

Figure 6 Swelling profile of uncoated and HA-coated PLGA scaffolds. Data are presented as mean (± s.d.). All measurements were analysed in triplicate.

a)

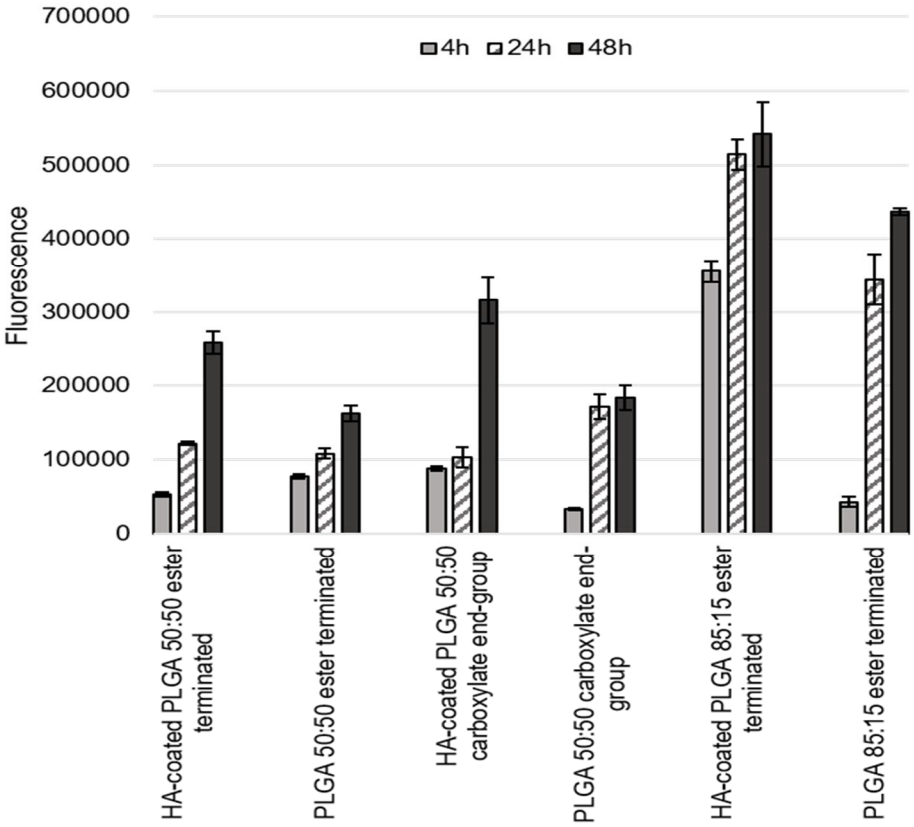

b)

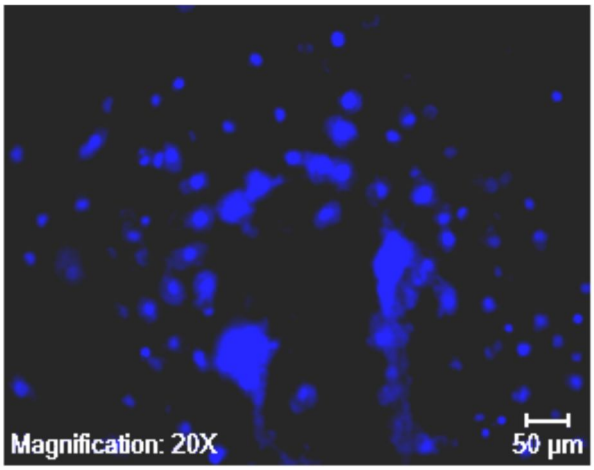

Figure 7: Cell viability of L929 cells at 4, 24 and 48 hours of culture (a) and live staining fluorescence of L929 cells on the surface of HA-coated PLGA 85:15 ester terminated scaffold (b). Data are presented as mean (± s.d.) and analysed using ANOVA followed by Student's T test. *p-value* < 0.05 was considered to be significant. All measurements were analysed in triplicate.

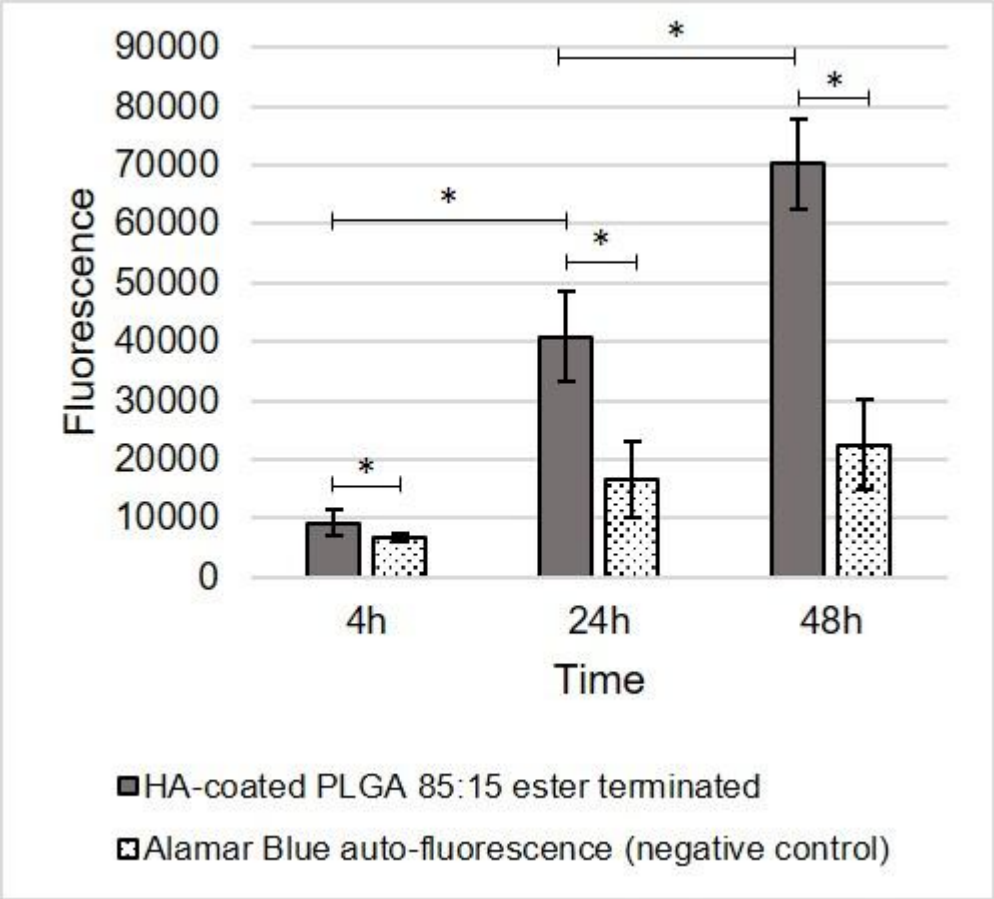

Figure 8: Cell viability of MCF-7 cells on HA-coated PLGA 85:15 ester terminated scaffolds at 4, 24 and 48 hours after microfluidics incubation. Data are presented as mean (± s.d.) and analysed using ANOVA followed by Student's T test. *p-value* < 0.05 (*) was considered to be significant. All measurements were analysed in triplicate.